Journal of Power Sources 244 (2013) 614–619

Contents lists available at SciVerse ScienceDirect

Journal of Power Sources

journal homepage: www.elsevier.com/locate/jpowsour

Short communication

Functional binder for high-performance Li–O_2 batteries

Yanming Cui, Zhaoyin Wen*, Yan Lu, Meifen Wu, Xiao Liang, Jun Jin

CAS Key Laboratory of Materials for Energy Conversion, Shanghai Institute of Ceramics, Chinese Academy of Sciences, Shanghai 200050, PR China

HIGHLIGHTS

- Conductive polymer PPy was introduced as functional binder for cathode of Li–O_2 cell.
- PPy binding cathode demonstrates lower contact/charge-transfer resistance than PVDF.
- PPy promotes simultaneous Li^+/e^- transfer in cathode during the discharge/charge.
- PPy/C improves efficiency, specific capacity, rate capability and cycling stability.
- Cathode with PPy binder demonstrates a better integrity than the conventional PVDF.

GRAPHICAL ABSTRACT

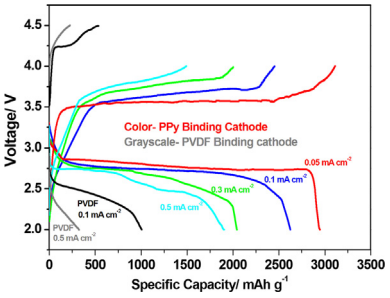

ARTICLE INFO

Article history:
Received 27 September 2012
Received in revised form
12 December 2012
Accepted 30 December 2012
Available online 29 January 2013

Keywords:
Polypyrrole
Binder
Air electrode
Lithium–air batteries

ABSTRACT

In the present work, the polypyrrole (PPy), as a conductive polymer, is for the first time introduced as functional binder of air cathode for lithium–oxygen batteries by a self-assembly process. Most of the carbon particles in the air cathode are found to be uniformly congregated with each other by the *in-situ* polymerized conductive polymer PPy, which affords a lower electrode resistance and higher electrode integrity. Replacement of the conventional inactive PVDF binder by the functional conductive polymer in the cathode, which not only acts as the binder and conductor, but also functions as a host for fast Li-ion insertion/extraction, has demonstrated its effectiveness in improving the cycle-efficiency, specific capacity, rate capability and cycling stability of the lithium–oxygen cells. In comparison with the PVDF binder, the PPy/C cathode demonstrates ~2.6 times (2626.3 mA h g^{-1} *vs.* 1005.8 mA h g^{-1}) and ~5.3 times (1816.4 mA h g^{-1} *vs.* 345.6 mA h g^{-1}) higher capacity at 0.1 mA cm^{-2} and 0.5 mA cm^{-2} respectively.

1. Introduction

Li–air batteries have attracted more and more attention. Although much larger capacities are achieved than those of the common Li-ion batteries, excessively high overpotential, poor rate capability and bad cycling stability limit their practical use [1]. Although many works have been devoted to optimize the active materials in the cathode of the Li–O_2 batteries, such as carbon [2–4] and catalytic materials [5–9], there are few reports on the effects of the binder for the oxygen cathode.

The primary role played by the binder is to link different types of small particles together and to ensure the active material adhesion to the current collector of the cathode during subsequent cycling. However, the common binders used for the oxygen cathode of the lithium–oxygen cells are polyvinylidene fluoride (PVDF) or polytetrafluoroethylene (PTFE), which have strong binding strength, but low flexibility and moreover are readily swollen, gelled, or dissolved by the nonaqueous liquid electrolytes especially at elevated

* Corresponding author. Tel.: +86 21 52411704; fax: +86 21 5241 3903.
E-mail address: zywen@mail.sic.ac.cn (Z. Wen).

0378-7753/$ – see front matter © 2013 Published by Elsevier B.V.
http://dx.doi.org/10.1016/j.jpowsour.2012.12.117

temperatures [10,11]. As a result of swelling or dissolving, adhesion among electrode particles and of the electrode materials to the current collector gradually deteriorated during repeated volume changes along with subsequent deposition/decomposition of the discharge products. Especially as the charge process is not completed, the undecomposed discharge products accumulating gradually in pores of cathode would further exacerbate the volume expansion effect, which would cause an increase in the contact resistance of electrode and hence capacity fading and cycle life shortening [7,12], similar to that in sulfur cathode [13,14] and Si anode [15,16]. Besides, the organic solvents (such as N-methyl-2-pyrrolidone) employed to dissolve PVDF would cause problems of safety and pollution [17].

For the insulating nature of the discharge products in the oxygen cathode, the redox reactions and electron transfer reactions can only occur at the surface [18]. As known, the conventional PVDF or PTFE are non-conductive, and the lack of facile transfer networks for electron/Li^+ in the carbon cathode with the conventional binder would limit the capacity, rate capability and cycle efficiency of the lithium–oxygen cells [19]. Conducting polypyrrole (such as PPy) has already been introduced into $LiMn_2O_4$ [20] and $LiFePO_4$ [21–23] based composite cathodes as the functional binder, and modestly improved capacities and rate capabilities were achieved. PPy is an important conducting polymer which we have introduced to substitute the oleophilic carbon material as an alternative of the conductive matrix in the oxygen cathode for high-performance Li–O_2 cells [24]. The conducting PPy polymer is electrochemically active in the voltage range of the operative redox (4–2 V *vs.* Li/Li^+) of the aprotic oxygen species [25]. So the PPy can not only act as an electrical conducting agent and binder for the cathode, but also function as a host material for fast Li^+ insertion/extraction/provide during a charge/discharge process [21–23]. Therefore, we expect particular functions of the PPy binder in the oxygen cathode during the cell process. In this present work, the PPy binding cathode (PPy/C) is realized by an *in-situ* self-assembly method and compared with the conventional PVDF binding one.

2. Experimental

2.1. Synthesis of the composite

The self-assembly process was realized by a simultaneously chemical polymerization of the monomer of pyrrole in the presence of a carbon support. PPy was polymerized from pyrrole with ammonium peroxydisulfate $(NH_4)_2S_2O_8$ as oxidizer in deionized water.

First, an aqueous suspension of 1.1 g ultrafine acetylene black carbon particles (AB, ~100 nm in diameter) with 500 mL 1 M HCl was sonicated for 60 min; then the Py monomer (1.5 g) was dissolved in the suspension and stirred magnetically at room temperature for 0.5 h and at 0 °C for 1 h. A precooled aqueous solution of $(NH_4)_2S_2O_8$ with 1 M HCl that acts as an oxidant was dropwisely added into the above solution. The mixture was reacted for 12 h at 0 °C. The precipitate was obtained by filtration, washed extensively with deionized water and ethanol separately, and finally dried at 80 °C overnight in vacuum.

2.2. Characterization of the PPy/C

The morphology of the synthesized samples was observed on a field emission scanning electron microscope (FESEM JSM-6700F). The structure of the samples was characterized by Powder X-ray diffraction (XRD, Rigaku RINT-2000) and Fourier Transform Infrared Spectroscopy (FTIR, Tensor 27). The N_2 sorption measurement was performed using Micromeritics Tristar 3000 at 77 K, and specific surface area was calculated using the Brunauer–Emmett–Teller (BET). The weight ratio of the polymer in the composite was analyzed by thermogravimetric analysis (TG-DSC, NET25CH).

2.3. Preparation of electrodes and Li–O_2 cells assembling configuration

The prepared composites (PPy/C) were mixed with AB and polyvinylidene fluoride (PVDF, in N-methyl-2-pyrrolidone) (75:10:15 wt %) to fabricate the cathodes. The cathode was formed by casting the slurry mixture of PPy/C, AB and PVDF onto the aluminum current collector. Conventional PVDF-binding electrode was also prepared for comparison, which was formed with the mixture of the AB as supports and PVDF as binders with the same weight ratio of 11:15 according to the procedure described elsewhere [26,27]. In order to make the weight ratio of binder material close to that in the PPy/C based electrode and demonstrate the disadvantage of PVDF more clearly, the high content of PVDF (58 wt %) was decided to be taken in the conventional PVDF binding electrode. All the air electrodes were subsequently dried in vacuum at 100 °C for 12 h prior to use. The mass loadings of PPy/C and PVDF electrodes were 11 ± 0.05 mg cm^{-2} and 10 ± 0.08 mg cm^{-2}, respectively. The average electrode thickness for all electrodes was 500 ± 30 μm.

The electrochemical activities of the composites for the discharge and charge steps were examined in Li–O_2 cells. The electrochemical cells used were based on the Swagelok Cell design composed of a Li metal anode (14 mm in diameter, 0.25 mm in thickness), an electrolyte (LITFSI in DME), Celgard 2400 separator, and the as-prepared cathode. The cells were operated at 1 atm of DME-saturated O_2 in a vessel of 5000 ml. It is noticed that dimethoxyethane (DME) was employed as the electrolyte solvent, because there is no verifiably stable electrolyte yet and DME was reported to be more stable than carbonated ones [28] and have high O_2 solubility [29]. Cells were tested in the voltage range of 2.0–4.0 V (*vs.* Li/Li^+) at the current densities of 0.05, 0.1, 0.3, 0.5 mA cm^{-2}. Specific capacities of PPy/C electrode were normalized by the total weight of the carbon (AB that in the composite and that as the additive) and PPy in the electrode (that is 95% of total mass of the cathode), and PVDF-binding cathode by weight of the carbon (42.3% of total mass of the cathode).

3. Results and discussion

With the *in-situ* polymerized PPy in the solution dispersed with fine AB particles, a uniform distribution of carbon as support and conductive PPy polymer as binder in the composite (PPy/C) was obtained. The AB was employed in this study because of its ultrafine feature (Fig. 1a). As the SEM images in Fig. 1b shown, the carbon particles are uniformly incorporated in the PPy polymer matrix. Most of the electrode particles are congregated with each other by the sticky polymers. Because the similar particle morphologies of both the carbon material and PPy binder, it is difficult to distinguish the PPy from the AB.

The XRD patterns and FTIR spectra in Fig. 2a and b clearly demonstrate the formation of PPy in the composite. The XRD patterns (Fig. 2a) of PPy/C composite demonstrate lower intensities of carbon's (002) and (100) peaks than those in pristine AB, which would be induced by the coating or cross-linking of the PPy on the carbon surface. FTIR spectra of the prepared PPy and PPy/C are characterized by the fundamental vibrations of pyrrole ring centered around 1545 cm^{-1} and 1458 cm^{-1}. The 1291 cm^{-1} and 1043 cm^{-1} peaks corresponding to the in-plane vibration of =C–H, and the 1175 cm^{-1} peaks corresponding to the –C–N stretching

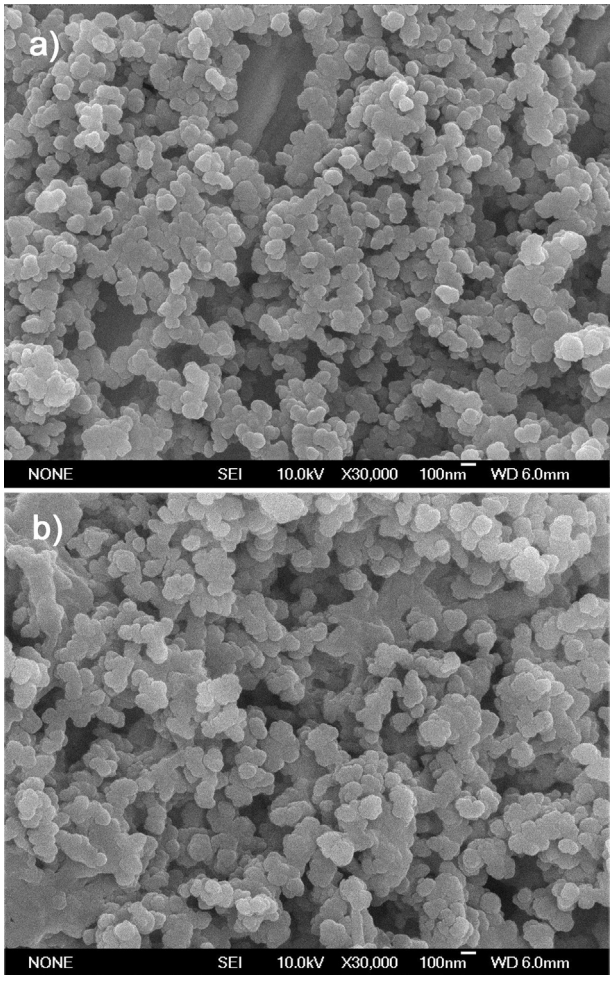

Fig. 1. SEM images of (a) AB and (b) the PPy/C composite prepared by a self-assembly method.

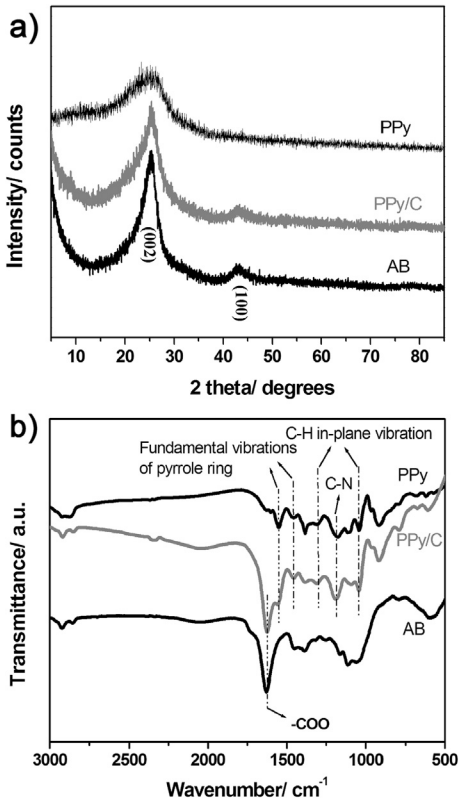

Fig. 2. XRD patterns (a) and FTIR spectra (b) of the PPy/C composite.

vibration are also observed [30]. The peak at 1628 cm^{-1} could be related to the AB involved in composite.

Fig. 3 shows the TG-DSC profiles of the prepared PPy/C composite, pure PPy and AB. The decomposition of PPy begins at around 300 °C and completes at about 600 °C. Because the weight loss of the AB before 600 °C can be ignored, the weight ratio of the polymer in the PPy/C can be approximately calculated according to the weight loss of the composite before 600 °C. The weight ratio of ~45 wt% of PPy in the composite was therefore obtained.

BET results are shown in Fig. 4. The PPy/C composite demonstrates a little lower specific surface area and pore volume (46.31 $m^2\ g^{-1}$ and 0.07596 $cm^3\ g^{-1}$) than those of the precursor of AB (65.29 $m^2\ g^{-1}$ and 0.1107 $cm^3\ g^{-1}$), which could be associated with the binding effects of PPy in the composite.

In order to evaluate the improved electronic conductivity of cathode by the conducting polymer as binder, electrochemical impedance spectroscopic analyses (EIS) were conducted on the whole Li–O_2 cells based on PPy/C and PVDF at initial stage of the discharge, as shown in Fig. 5. It has been proved that the contribution of the anode impedance to the whole Li–O_2 cell is so small that the major source of the cell impedance comes from the cathode [12]. The impedance spectra are composed of a semi-circle in the high frequency region corresponding to the contact resistance and charge transfer resistance, as well as an inclined line in the low frequency region related to the mass diffusion within the air electrodes. The EIS results of the two cells demonstrate that the cell with PPy binder exhibits a substantially smaller interface resistance and charge transfer resistance than that with conventional PVDF binder. The results confirm the positive effect of the highly conductive network made of PPy binder with repaired incomplete carbon network [31], indicating PPy as a promising binder for the cathode of a high energy density lithium–air battery.

The galvanostatic discharge and charge results of the Li–O_2 cells with PPy/C based cathode compared to conventional PVDF binding one at different current densities of 0.05 and 0.1 mA cm^{-2} are shown in Fig. 6. As seen, the as-prepared PPy/C based cathodes demonstrated quite distinct discharge/charge profiles from the conventional PVDF based one. At a low current of 0.05 mA cm^{-2}, the catalyst free PPy/C displayed a discharge voltage plateau at as high as ~2.79 V (~0.4 V consistently higher than the PVDF one),

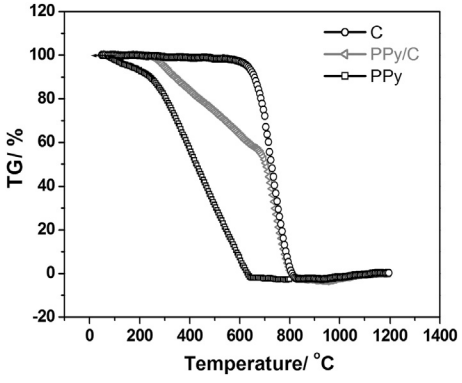

Fig. 3. TG profile of the PPy/C composite.

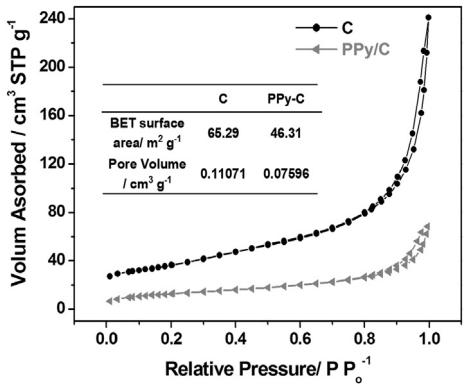

Fig. 4. BET results of the PPy/C composite.

and a charge voltage of as low as ~3.57 V (~0.5 V consistently lower than the PVDF one). At 0.1 mA cm^{-2}, the much higher discharge voltage (~2.75 V) and lower charge voltage (~3.65 V) than those of the PVDF based one (~2.5/4.25 V) were also obtained. The PPy/C based cathode is also found to exhibit more than 2 times higher specific discharge capacities even normalized by the mass of both the support and binder (95 wt% of the total electrode), compared to those of the PVDF binding electrode by only support (42.3 wt% of the total electrode), at 0.05 mA cm^{-2} of 2952.8 *vs.* 1916.5 mA h g^{-1} and at 0.1 mA cm^{-2} of 2626.3 mA h g^{-1} *vs.* 1005.8 mA h g^{-1} respectively. It is noticeable that the PPy/C demonstrates a lower BET surface area but a higher capacity. One of the reasons could be the PPy here not only functions as the binder but also a simultaneous Li^+ and e^- conductive matrix favorable for the deposition of more discharged products [31,32].

We then examine the effects of higher current densities on the discharge/charge performance of the PPy/C based Li–O_2 cells as shown in Fig. 7. The cell exhibits surprisingly high rate capability, demonstrating capacity retentions of 88.94% at 0.1 mA cm^{-2}, 69.09% at 0.3 mA cm^{-2} and 64.2% at 0.5 mA cm^{-2} of the capacity at 0.05 mA cm^{-2} *vs.* only 52.48% at 0.1 mA cm^{-2} and 18.03% at 0.5 mA cm^{-2} of the PVDF binding cathode. Very high discharge platforms are realized in the PPy/C based cathode, ~2.79 V at 0.05 mA cm^{-2}, ~2.75 V at 0.1 mA cm^{-2}, ~2.72 V at 0.3 mA cm^{-2} and even as high as ~2.70 V at 0.5 mA cm^{-2}, indicating very low polarization in the cell. It is worthy to note that both the discharge and charge processes of PPy/C undergo two stages, which becomes more apparent at higher current densities: 1) The discharge voltage at the beginning stage is higher with a flat platform. While at the second stage, the discharge voltage decreases more quickly,

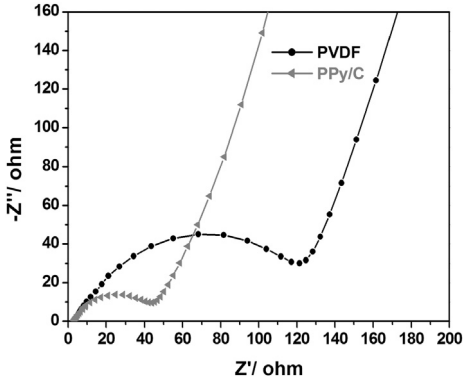

Fig. 5. AC impedance spectroscopy of the different electrodes in Li–O_2 cells.

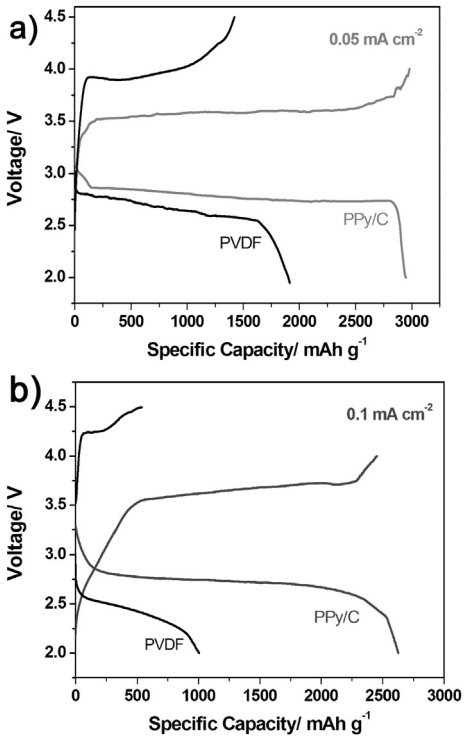

Fig. 6. The galvanostatic charge and discharge profiles of the PPy/C and conventional PVDF based Li–O_2 cells at (a) 0.05 mA cm^{-2} and (b) 0.1 mA cm^{-2}.

resulting in a sloping discharge profile (such as at the higher current density of 0.5 mA cm^{-2} after 500 mAh g^{-1}), which is much more like the common discharge profiles of the lithium–oxygen cells reported at higher currents. 2) The charge voltage in the first stage of charge process is lower and gradually increased without an apparent plateau, and the profile shape is similar to that of the electrochemically active PPy. The first stages in both the discharge and charge process are supposed to be associated with the cell reaction between the Li^+ and electrochemically active PPy at the initial discharge/charge process, which can be seen as the fast Li^+ insertion/extraction in PPy matrix. The corresponding capacity is higher than the theoretic value of PPy (~100 mAh g^{-1}), indicating some Li–O_2 reaction was also involved. According to the profile shapes and as far as the author known, as well as the previous works in the PPy/$LiFePO_4$ [21–23], the improved capacity, high discharge voltage and low charge voltage of the PPy/C are supposed to be induced by the PPy binder which serves as the host to promote both the e^-/Li^+ transfer in the cathode [21–23] and decreases

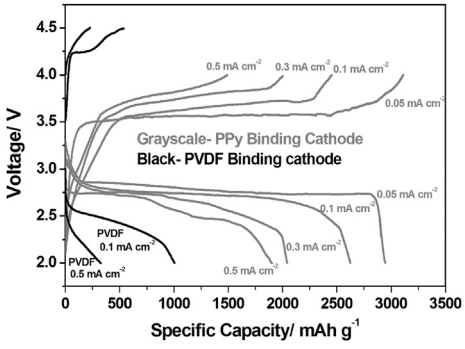

Fig. 7. The rate capability of the Li–O_2 cells with PPy/C and PVDF based electrodes.

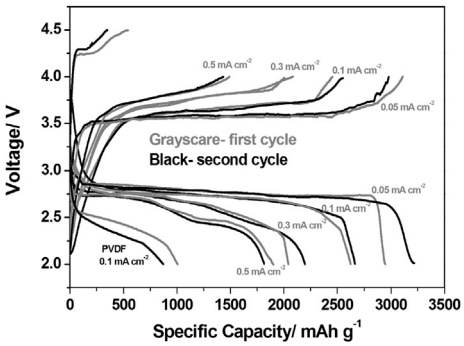

Fig. 8. The cycling performance of the Li–O_2 cells with PPy/C and PVDF based electrodes at 0.05, 0.1, 0.3, 0.5 mA cm^{-2}.

the cathode resistance as the formation/decomposition of the solid products during the discharge/charge process, especially at higher currents when resistance of Li^+ diffusion in the solid ORR products and in DME electrolyte greatly increased [18,19,28]. Besides the kinetic effect, the high polarity of the PPy could also be an important reason [24], which would help to achieve a larger three-phase interface in the low polarized electrolyte [2,33].

Considering the high volatility of the electrolyte solvent, only the second charge/discharge profiles are shown together with those of the first cycle in Fig. 8. Little deviation of the platforms in the second cycle was observed from the first cycle at different rates, indicating the high reversibility of the PPy/C based air electrode and stably functional activities of the PPy binder. While the second cycle of the conventional PVDF binding cathode, typically at 0.1 mA cm^{-2}, shows obviously decreased discharge voltage and increased charge voltage. The improved cycling stability of the PPy/C could be attributed to the efficient binding ability of the PPy in maintaining good contacts among particles in the electrode and ensuring sufficient adhesion of the electrode material to the current collector along with the sustainable deposition/decomposition of the cathode discharged products, which can be proved in discharged electrode of Fig. 9a with alleviated volume expansion [12]. On the contrary, cracks are clearly observed in the discharged PVDF binding electrodes after the sustainable deposition of discharge products as shown in Fig. 9b, which would gradually lead to the loss of electrical contact, the increase of interfacial resistance and the fade of the cycling performance as observed in previous works [7,12].

The PPy here not only functions as an efficient binder, but also increases the electrical conductivity and enhances the Li^+ transfer in the cathode, which affords the cathode with well improved performance of cycle-efficiency, specific capacity, rate capability and cycling stability. It is worth to point out that the functional binder is not limited to PPy, and other conducting polymers are also expected to have the similar functional effects.

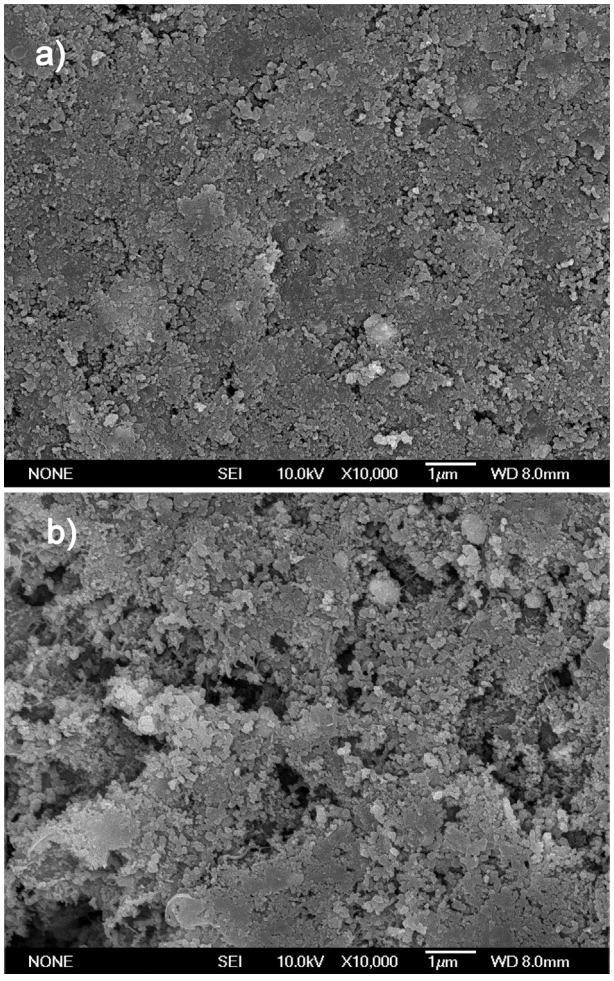

Fig. 9. SEM images of the (a) PPy/C and PVDF (b) electrodes after full discharge.

4. Conclusions

In the present work, the conductive polymer polypyrrole (PPy) was for the first time introduced to the air electrode as a functional binder by an *in-situ* self-assembly process. The PPy/C based electrode demonstrates improved cycle-efficiency, specific capacity, rate capability and cycling stability. The improved performances of the PPy/C based air electrode are attributed to the effects of the PPy in increasing electronic conductivity, integrating the components of the electrode and tying up the electrode to the current collector, alleviating the electrode volume expansion during the sustainable deposition/decomposition of the discharge products. Moreover, it also serves as a host for fast Li-ion insertion/extraction in the electrode. The employment of the functional binder as an alternative of the conventional PVDF paves a new way to develop high-performance lithium–air batteries.

Acknowledgment

This work was financially supported by NSFC Project No. 50730001 and research projects from the Science and Technology Commission of Shanghai Municipality No. 08DZ2210900.

References

[1] R. Padbury, X. Zhang, J. Power Sources 196 (2011) 4436–4444.
[2] C. Trana, X.-Q. Yang, D. Qu, J. Power Sources 195 (2010) 2057–2063.
[3] P. Kichambare, J. Kumar, S. Rodrigues, B. Kumar, J. Power Sources 196 (2011) 3310–3316.
[4] X.H. Yang, P. He, Y.Y. Xia, Electrochem. Commun. 11 (2009) 1127–1130.
[5] A. Débart, J. Bao, G. Armstrong, P.G. Bruce, J. Power Sources 174 (2007) 1177–1181.
[6] H. Cheng, K. Scott, J. Power Sources 195 (2010) 1370–1374.
[7] Y. Cui, Z. Wen, Y. Liu, Energy Environ. Sci. 4 (2011) 4727–4734.
[8] Y. Cui, Z. Wen, S. Sun, Y. Lu, J. Jin, Solid State Ion. 225 (2012) 598–603.
[9] Y. Lu, Z. Wen, J. Jin, Y. Cui, M. Wu, S. Sun, J. Solid State Electrochem. 16 (2012) 1863–1868.
[10] A. Magistris, P. Mustarelli, F. Parazzoli, E. Quartarone, P. Piaggio, A. Bottino, J. Power Sources 97 (2001) 657–660.
[11] S.S. Zhang, T.R. Jow, J. Power Sources 109 (2002) 422–426.
[12] M. Mirzaeian, P.J. Hall, J. Power Sources 195 (2010) 6817–6824.
[13] M. He, L.-X. Yuan, W.-X. Zhang, X.-L. Hu, Y.-H. Huang, J. Phys. Chem. C 115 (2011) 15703–15709.
[14] L.A. Montoro, J.M. Rosolen, Solid State Ion. 159 (2003) 233–240.

[15] D. Munao, J.W.M. van Erven, M. Valvo, E. Garcia-Tamayo, E.M. Kelder, J. Power Sources 196 (2011) 6695–6702.
[16] B. Koo, H. Kim, Y. Cho, K.T. Lee, N.-S. Choi, J. Cho, Angew. Chem. Int. Ed. 51 (2012) 8762–8767.
[17] Z.P. Cai, Y. Liang, W.S. Li, L.D. Xing, Y.H. Liao, J. Power Sources 189 (2009) 547–551.
[18] M.D. Radin, J.F. Rodriguez, F. Tian, D.J. Siegel, J. Am. Chem. Soc. 134 (2012) 1093–1103.
[19] P. Albertus, G. Girishkumar, B. McCloskey, R.S. Sánchez-Carrera, B. Kozinsky, J. Christensen, A.C. Luntz, J. Electrochem. Soc. 158 (2011) A343–A351.
[20] A.D. Pasquier, F. Orsini, A.S. Gozdz, J.M. Tarascon, J. Power Sources 81 (1999) 607–611.
[21] Y.-H. Huang, J.B. Goodenough, Chem. Mater. 20 (2008) 7237–7241.
[22] K.-S. Park, S.B. Schougaard, J.B. Goodenough, Adv. Mater. 19 (2007) 848–851.
[23] T. Tamura, Y. Aoki, T. Ohsawa, K. Dokko, Chem. Lett. 40 (2011) 828–830.
[24] Y. Cui, Z. Wen, X. Liang, Y. Lu, J. Jin, M. Wu, X. Wu, Energy Environ. Sci. 5 (2012) 7893–7897.
[25] P. Novák, K. Müller, K.S.V. Santhanan, O. Haas, Chem. Rev. 97 (1999) 207–281.
[26] J. Read, J. Electrochem. Soc. 149 (2002) A1190–A1195.
[27] M. Leskes, N.E. Drewett, L.J. Hardwick, P.G. Bruce, G.R. Goward, C.P. Grey, Angew. Chem. Int. Ed. 51 (2012) 8560–8563.
[28] R.R. Mitchell, B.M. Gallant, C.V. Thompson, Y. Shao-Horn, Energy Environ. Sci. 4 (2011) 2952–2958.
[29] J. Read, K. Mutolo, M. Ervin, W. Behl, J. Wolfenstine, A. Driedger, D. Foster, J. Electrochem. Soc. 150 (2003) A1351–A1356.
[30] M. Sun, S.C. Zhang, T. Jiang, L. Zhang, J.H. Yu, Electrochem. Commun. 10 (2008) 1819–1926.
[31] W.-M. Chen, L. Qie, L.-X. Yuan, S.-A. Xia, X.-L. Hu, W.-X. Zhang, Y.-H. Huang, Electrochim. Acta 56 (2011) 2689–2695.
[32] A. Javier, S.N. Patel, D.T. Hallinan Jr., V. Srinivasan, N.P. Balsara, Angew. Chem. Int. Ed. 50 (2011) 9848–9851.
[33] W. Xu, J. Xiao, D. Wang, J. Zhang, J.-G. Zhang, J. Electrochem. Soc. 157 (2010) A219–A224.